https://doi.org/10.20965/jrm.2012.p0133

Paper:

On-Demand and Size-Controlled Production of Droplets by Magnetically Driven Microtool

Lin Feng*, Tomohiro Kawahara*, Yoko Yamanishi*, Masaya Hagiwara*, Kazuhiro Kosuge, and Fumihito Arai***

*Dept of Micro-Nano Systems Engineering, Nagoya University
Furo-cho, Chikusa-ku, Nagoya 464-8603, Japan
E-mail: f-lin@biorobotics.mech.nagoya-u.ac.jp
**Tohoku University
6-6-01 Aza-aoba, Aramaki, Aoba-ku, Sendai 980-8579, Japan
[Received June 9, 2011; accepted August 16, 2011]

We have successfully produced size-controlled emulsion droplets on a chip by adjusting the vibration frequency for MMT. The novelty of this work is the fabrication of a thin coplanar Au electrode on the substrate of a microchip to work as a microsensor, and this microsensor contributed to a droplet-generation system with size estimation. When a droplet passes through the microsensor in the microchannel, it causes a change in the capacitance across a pair of microelectrodes in the microchannel, depending on the size of the droplet. We monitored the change in impedance in real time. The microsensor provided an output voltage proportional to the size of the droplet. The sensor output was observed by an oscilloscope at the primary stage. Manually we estimated the size and set a new actuation frequency for MMT to achieve on-demand and size control of the droplet. Real-time droplet detection was applied in this system. By monitoring the actuation frequency for MMT, size-controlled and on-demand droplet generation could be successfully carried out.

Keywords: droplet dispensing, magnetically driven microtool, robot-on-a-chip, impedance sensor

1. Introduction

The emulsification of liquids is an emerging technology [1], such as encapsulation of DNA [2], drug-delivery system for nanoparticles [3], and single-molecular enzyme analysis [4]. Since emulsification has become a crucial industrial technique, the quality of the emulsion droplets is significant, especially in biotechnology and nanomedicine applications [5]. In the last decade, droplets have been extensively used by various industries for plastic polymerization drug development, and chemical processing [6]. Recently, droplets have been enabled for microfluidic technologies to be used as liquid-reaction vessels for protein crystallization screening [7], as templates for providing self-assembly of materials [8, 9], as moulds for forming polymeric microspheres [10, 11], and as components for microelectrical actuation [12]. Many researchers have already studied the highly efficient droplet generation [13–15]. Sung-Yong Park et al. (2011) demonstrated an approach for on-demand high-speed droplet generation driven by pulse laser-induced cavitation [16]. The actuation mechanism of droplet generation is based on pulse laser-induced, rapidly expanding cavitation vapor bubbles that enable on-demand droplet generation at a super-high speed. However, the system setup is based on a laser system, which has the shortcomings of a huge instrument with complicated manipulation and high cost. Moreover, the estimation of droplet size is performed by a visual system, which is controlled by an open-loop size-control system with the same issues as the laser system.

We have developed novel on-demand and size-controlled method for producing emulsion droplets by magnetically driven microtools (MMT). MMT settled in a PDMS microfluidic chip shows the advantage of disposability and non-contamination. The concept view of the microchannel is shown in **Fig. 1(a)**. An MMT actuated laterally by non-contact magnetism can be made to act as "chopper" disintegrating a multiphase flow and controlling droplet size actively and on-demand. For the present research, two pairs of microsensors are installed at the outlet microchannel to detect the droplet and calculate the droplet size and velocity. In order to generate a compatible size of droplets on the dispensing chip we compared the actual droplet size with the desired size, and determined the force for adjusting the size of dispensing droplets. By using this method, the size distribution errors can be eliminated, and desired sizes of the droplets are obtained.

2. Concept of New Droplet Generation

2.1. Concept of On-Demand and Size-Controlled Chip

In our previous study, we developed low-cost mass-produced MMT, which provided many actuating func-

tions such as sorting, valve operation, and loading [17, 18]. **Figs. 1(a)** and **(b)** show the concept view of droplet generation chip, an MMT was installed in the microchamber, and the hydrophobic and hydrophilic flows entered from yellow and blue inlets, respectively. The design was a parallel-plate structure with two outlets, where a drain port between two outlets was always closed and only used at the initial stage for removing the bubbles, and it was closed during the droplet-dispensing experiment. First, we evaluated the displacement of MMT to confirm that the lateral motion of MMT is enough to close the channel. The calculation of a simple bending of the MMT legs indicated that the displacement of MMT actuated by the magnetic flux density of a permanent magnet (102 mT) was 902 μm and this displacement was larger than the width of the microchannel (150 μm). Thus, the lateral motion of MMT is always restricted by the microchannel wall. **Fig. 1(c)** shows that the height of the microchannel for a hydrophobic fluid was off from the upper level of the hydrophilic fluid microchannel. By utilizing a two-step exposure process, we made a trapezoidal structure for the microchannel. The height of the hydrophobic fluid microchannel was 75 μm, where the height of MMT was 100 μm and the heights of the chamber and outlet were 150 μm. A stratified microchannel with a staircase structure was fabricated for the current design to allow MMT playing a better role without leakage. **Fig. 2** shows the overview of the chip; MMT (black) had a parallel-plate structure. The chamber was sandwiched between two continuous phases. The two transparent microchannels shown in the figures are the olive-oil channels. The ethanol flows through the middle channel.

The mechanism of droplet generation is summarized as follows (**Figs. 1(a)** and **(b)**). When the MMT moves downward, it blocks the dispersed microchannel (75 μm) below. As the height of MMT is 100 μm, it could block the outlet of the dispersed phase completely. Therefore, the hydrophobic fluid (olive oil) has only one exit, which is the upper channel, to flow out. The same principle is used when MMT moves upward (**Fig. 1(b)**). Once MMT cuts the hydrophobic flow, a droplet is generated simultaneously. While the hydrophilic flow (ethanol dyed with methylene blue) leaks through the gap of MMT because of its low fluidic drag force, the droplet can be transported by the hydrophilic flow. Consequently, the on-demand and size-control production of droplets can be easily realized by using this novel hydraulic design on a chip. This hydraulic design balances the excess pressure on a chip efficiently and twice the number of size-controlled droplets can be produced at both sides of MMT. However, it is important to note that our final purpose is the measurement of droplet size and automatic size-controlled droplet generation by employing a microsensor.

2.2. Principle of Droplet Detection

Two pairs of coplanar electrode sensors were installed on the outlet microchannel at the substrate, which could work as detectors for droplet detection. These two sensors

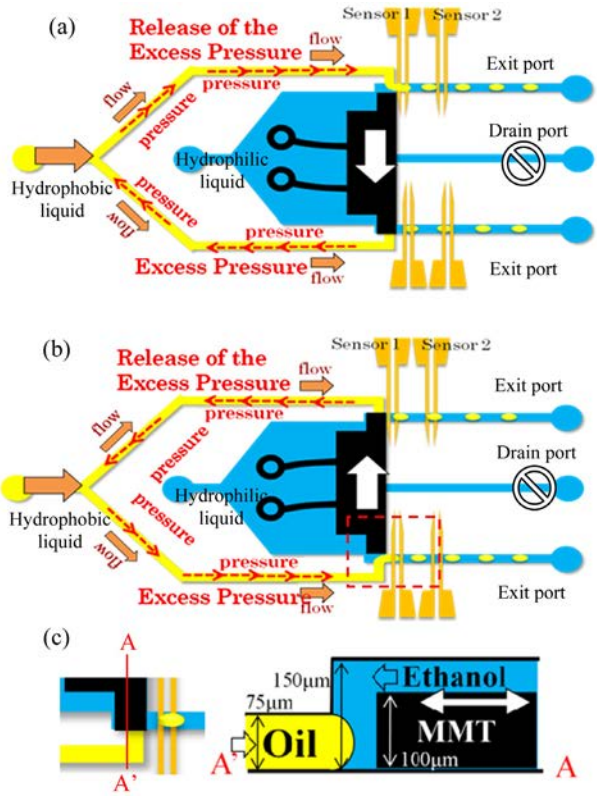

Fig. 1. Concept view of current on-demand and size-controlled droplet-dispensing design. (a) Striking droplet on the bottom, (b) striking droplet on the top, (c) trapezoidal structure of microchannel from a sectional view.

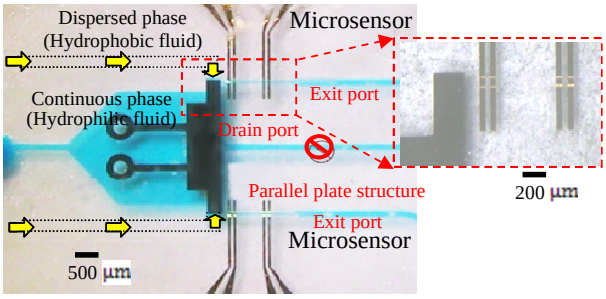

Fig. 2. Overview of fabricated on-demand and size-controlled droplet-dispensing chip.

were installed at the two outlets (**Fig. 2**), and they can be observed clearly in the magnified figure. When an olive-oil droplet passed through the two pairs of microsensors in the microchannel, a change in capacitance could be detected by the difference in permittivity between the olive oil and ethanol dyed with methylene blue [19]. The microsensor sensed the change in the differential capacitance and provided an output voltage proportional to the change in capacitance. The interval between the two microsensors was determined (1 mm) at an initial stage on the basis of the droplet detection principle, and thus, outflow rate and droplet size could be derived accurately. As shown in **Fig. 3**, we assumed that two coplanar and semi-infinite conducting films separated by a gap distance of $2a$ were embedded within a uniform dielectric medium of permittivity ε_r and each was maintained at a constant po-

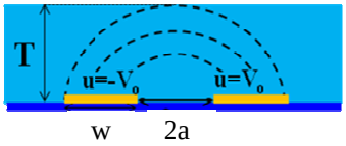

Fig. 3. Concept view of capacitance corresponding to a pair of semi-infinite electrodes.

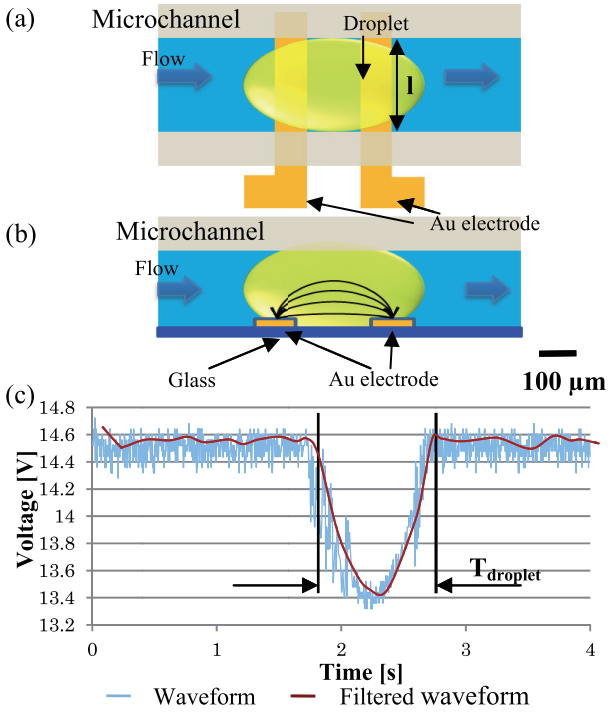

Fig. 4. Principle of sensing part. (a) Top view of sensing part, (b) side view of sensing part, (c) sensing result of a droplet (setting: AC 0.01 V, 10 kHz).

tential $\pm V_0$. The capacitance of an electrode pair of finite width w could be estimated by the following equation [20]

$$C = \frac{Q}{2V_0} = \frac{2\varepsilon_r \varepsilon_0 l}{\pi} \ln\left[\left(1+\frac{w}{a}\right) + \sqrt{\left(1+\frac{w}{a}\right)^2 - 1}\right] \quad (1)$$

where C is the capacitance, Q is the total charge on a single electrode, V_0 is constant potential maintained at the electrode pair, ε is the vacuum permittivity, w is an electrode pair of finite width and l is the length of the electrode pair for $l \gg w$. Thus, the capacitance changes because of different fluidic materials as their electric permittivity ε_r is different.

In **Fig. 3**, T is the field penetration depth, w is the finite width of the conducting plates, and u is the embedded load voltage in a dielectric liquid. In this case, T is estimated as 158 μm [20], which is greater than the microchannel height of 150 μm; therefore, the capacitance is only determined by the permittivity of different materials. **Fig. 4** shows the principle of sensing when a droplet is passing through the sensors. Here, droplet size can be estimated by the change in capacitance with time multiplied by the flow velocity. **Fig. 4(a)** shows the top view of the sensing part of the microchannel. **Fig. 4(b)** shows a side view of the microchannel, when an olive-oil droplet passes through the electrode array. The changes in the voltage of parallel electrodes are shown in **Fig. 4(c)**.

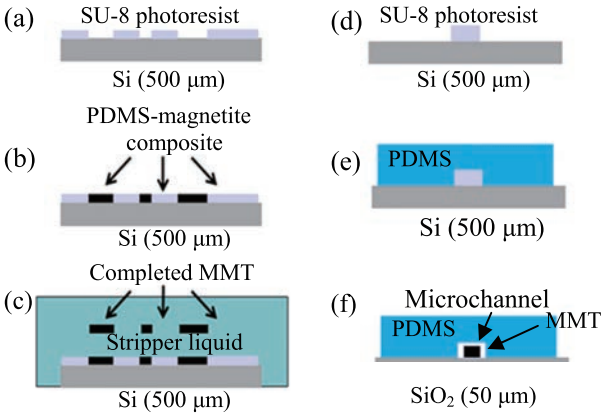

Fig. 5. Fabrication process for polymer-based MMT and microchannel.

3. Fabrication of Droplet-Generation Chip with Impedance Sensor

Figure 5 shows the fabrication process of polymer-based MMT and microchannel. The fabrication of MMT is summarized in the following steps: (1) a thick negative photoresist (SU-8, Nippon Kayaku Co., Ltd.) was pasted on the silicon substrate, and an MMT mold was produced by photolithography, (2) a mixture of PDMS and magnetite (Fe_3O_4, 50 wt%) was spread over the patterned mold and baked in an oven (110°C, 10 min), (3) MMT was obtained by carefully peeling off with tweezers, and (4) the surface of MMT was Teflon-coated with CF_4 gas by the plasma-ashing method (discharge power: 130 W) for 30 min to avoid any stiction in the microchannels. The average diameter of the magnetite particles (Fe_3O_4) was 200 nm. In the case of the microchannels, after making an SU-8 pattern as the mold, the pattern was transcribed to PDMS. The PDMS microchannel was obtained after baking in the oven (90°C, 20 min).

Figure 6 shows the fabrication process for the microsensor. To fabricate the electrodes, a glass plate was coated with 300 nm Cr and 300 nm Au. Moreover, the glass was coated with OAP (Tokyo Ohka Co., Ltd) for HMDS process, and then it was patterned by a positive photoresist OFPR (Tokyo Ohka Co., Ltd). After the photolithography and wet-etching process, the microsensor pattern was made on the glass substrate. Finally, OFPR was cleaned with acetone. The sensor wires were welded using Ag paste. Finally, we made the impedance sensor. MMT was placed in the microchamber of PDMS microchip, which was bonded with a glass substrate with the microsensors on it. **Fig. 7** shows the fabricated droplet-generation chip.

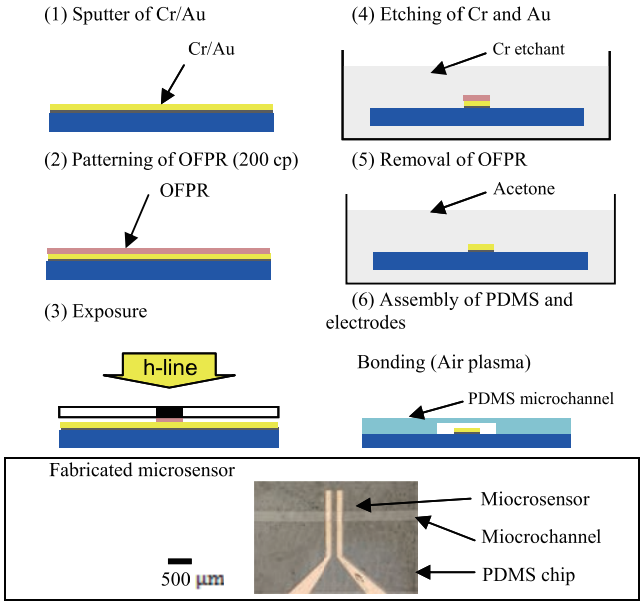

Fig. 6. Fabrication process for microsensor.

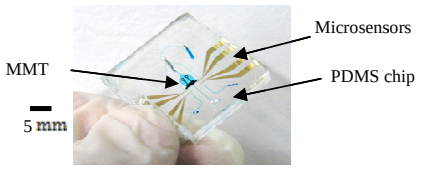

Fig. 7. Fabricated droplet-generation chip.

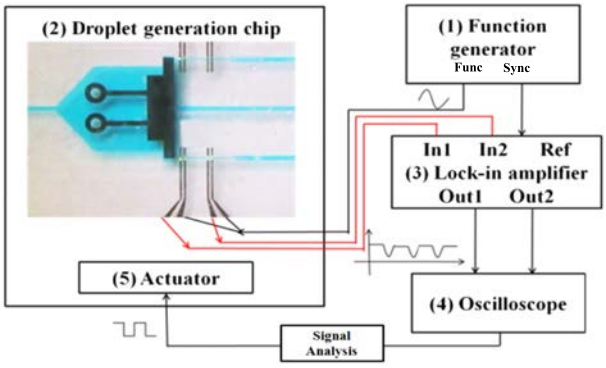

Fig. 8. Schematic of the experimental setup.

4. Experiment of Droplet Generation with Real-Time Droplet Detection

4.1. Overview of Experiment Setup

Figure 8 shows the experiment setup. The droplet generation system consisted of two critical modules: a droplet generation chip with an impedance sensor and a droplet real-time estimation module. The actuator of the droplet generation chip also consisted of two modules: an upper module containing a disposable microchannel and a lower actuation module (**Fig. 9**). The actuation module was composed of a magnetic circuit unit containing an electromagnetic coil and a permanent magnet unit. The magnetic flux density generated by the electromagnetic coil

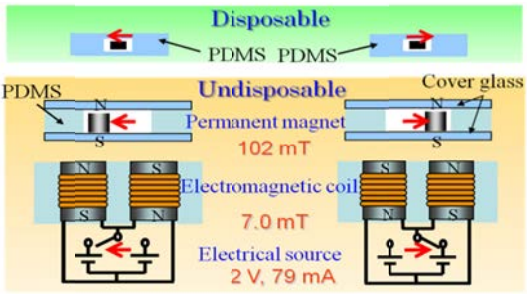

Fig. 9. Actuation construct of droplet-generation chip.

was amplified by the permanent magnet (neodymium) unit mounted between the microchannel and magnetic circuit, and MMT was moved by non-contact actuation. The direction of the current in the coil of the magnetic circuit could be switched to reverse the electromagnet's polarity, resulting in translational motion of the permanent magnet, and MMT also followed the translational motion.

For the first-step detection, we used a function generator (WF 1974, NF Corporation) by setting an output voltage $V_{p\text{-}p}$ of 0.01 V and frequency of 10 KHz with a sinusoidal waveform. The flow rate was set to 400 μm/s. Through two separate sets of digital lock-in amplifiers (LI 5640, NF Corporation) to the microsensor we obtained two different voltage values when ethanol and olive-oil were flowing. The voltage decreased when the olive-oil droplets flowed in the microchannel. Au parallel electrode provided different voltage signals under different flow conditions, as the conductivity was different. After analog-digital conversion, the voltage signal was directed to a computer. Through voltage-signal analysis, a new frequency signal was provided to the actuator, and hence, the variable size of the droplets could be produced automatically.

4.2. Size-Controlled Droplet Generation over a Wide Range

Figure 10 shows the photos of the droplet-dispensing experiment. The liquid for the dispersed phase was olive-oil and that for the continuous phase was ethanol dyed with methylene blue. The photos at the left-hand and right-hand sides in **Fig. 10** show droplet dispensing at the frequencies 2 Hz and 1 Hz, respectively, of MMT with the representative condition of droplet dispensing (oil: 0.02 ml/h; ethanol: 1 ml/h). **Fig. 11** shows the profile of the droplet size as a function of the MMT frequency. It was observed that we could obtain the droplets from the radius of 40 μm to 200 μm.

4.3. Basic Experiment Testing for Impedance Sensor

Figure 12(a) shows the basic experiment testing for the performance of the impedance sensor. We used five olive-oil droplets of different sizes passing through the microsensor in the microchannel; a change in the capacitance could be detected owing to the difference in

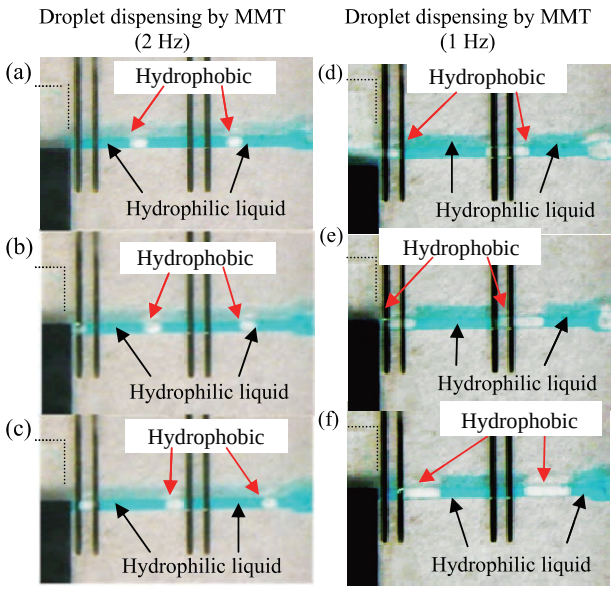

Fig. 10. Droplet dispensing by MMT. (Dotted line indicates microchannel for hydrophobic fluid).
(a), (d): Microchannel is open by MMT.
(b), (e): Olive-oil flow is cut by MMT.
(c), (f): Microchannel is closed by MMT.

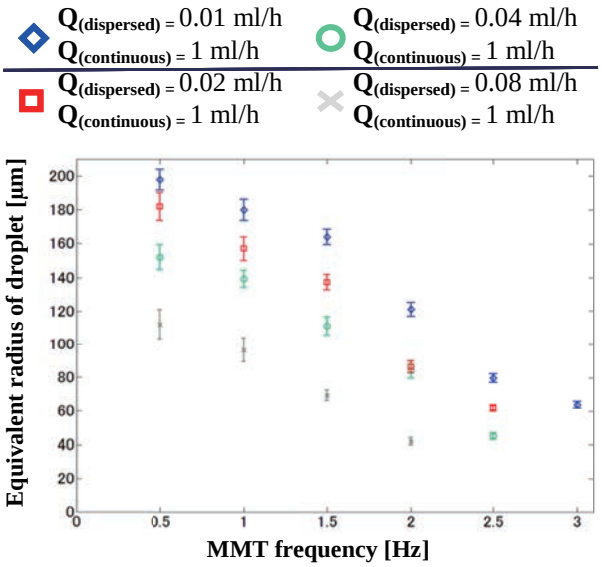

Fig. 11. Profiles of the droplet size as a function of the MMT frequency.

the permittivity between that of the olive-oil (2.5 F/m) and ethanol (24.3 F/m) (dyed with methylene blue). **Fig. 12(b)** shows that the impedance microsensor senses the change in the differential capacitance and provides an output voltage proportional to the change. To evaluate the relationship between the size of the dispensing droplet and the time span of voltage bandwidth, the equivalent droplet size was measured by CCD images. After the analysis of the data, the relationship between equivalent radius and time span of voltage could be confirmed from **Fig. 13**.

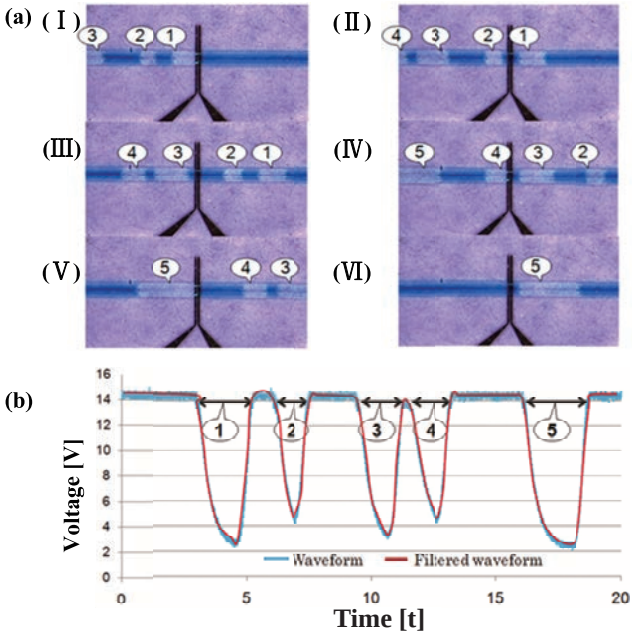

Fig. 12. Measured performance of the impedance microsensor. (a) Top view of the microchannel showing droplets passing over two coplanar electrodes. (b) Sensing result for the droplets performed in voltage format.

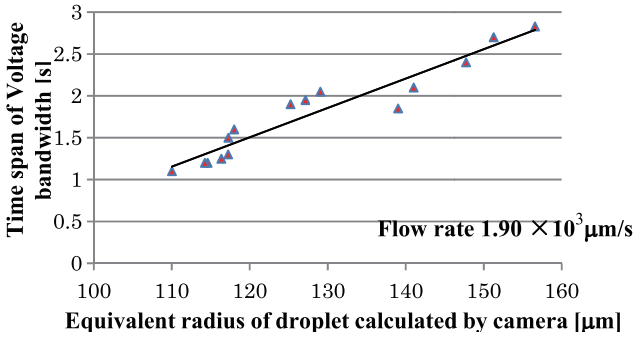

Fig. 13. Relationship between equivalent radius of droplet and time span of voltage bandwidth.

4.4. Experiment of Droplet Detection and Calculation

To confirm the principle of droplet detection, we first demonstrated a typical situation of dispensing droplets (**Fig. 14**). The droplets were flown through the microchannel-detection area under the conditions of a continuous phase flow rate of 0.01 ml/h and dispersed phase flow rate of 0.1 ml/h. Individual droplets were detected by measuring the impedance in the outlet microchannel part by an electrode pair. To capture tiny droplets, we made a thin slender microchannel at the detection part where the droplets can be deformed into a slim shape and can be detected easily. **Fig. 15** shows how the flow rate and droplet size can be calculated. In this case, we chose 11.5 V as the threshold voltage (**Fig. 15**), hence the velocity of outlet flow rate and droplet size could be

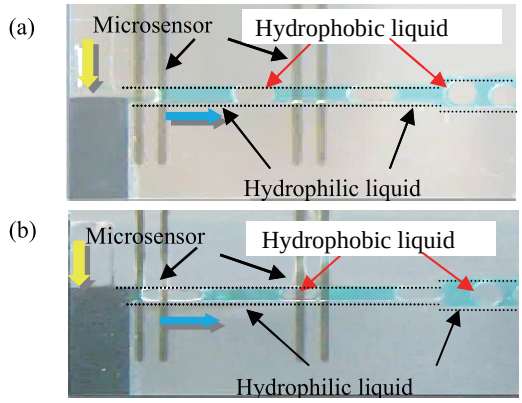

Fig. 14. Droplets were flowing through two pairs of electrodes.

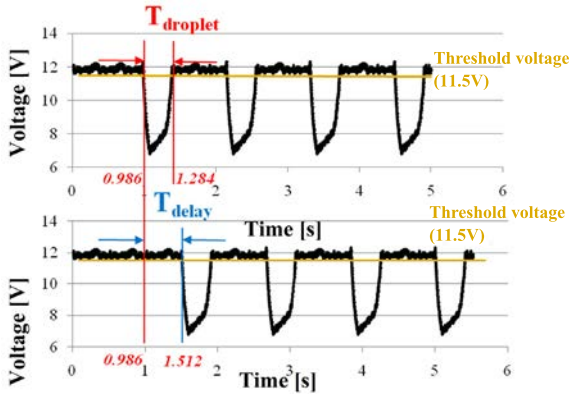

Fig. 15. Two voltage signals detected respectively by two pairs of electrodes.

deduced as follows:

$$V = \frac{D}{T_{\text{delay}}} \quad \ldots\ldots\ldots\ldots\ldots\ldots \quad (2)$$

where V is the outlet flow rate, D is the interval distance between two pairs of microsensors, and T_{delay} is the time delay for the same droplet, which was detected by two pairs of sensors. The output voltage signal was input to an oscilloscope (TDS3014, Tektronix), which can calculate the output voltage value accurately to microseconds. In this case, the distance between the two pairs of electrodes was 1×10^3 μm, and T_{delay} was 0.526 s as obtained by the oscilloscope; therefore, the flow rate V was deduced to be 1.9×10^3 μm/s. Hence, the length of the droplets can be derived by multiplying the flow rate with time:

$$L = V * T_{\text{droplet}} \quad \ldots\ldots\ldots\ldots\ldots\ldots \quad (3)$$

where L is the length of a droplet and T_{droplet} is the time span of a single droplet detected by one microsensor. The length of the droplet, in this case, was 5.67×10^2 μm. Consequently, the equivalent radius of the droplet could be estimated by the follow equation:

$$R = \delta * \sqrt[3]{\frac{3 * L * W * H}{4\pi}} + \alpha. \quad \ldots\ldots\ldots \quad (4)$$

In Eq. (4), R represents the equivalent radius of a droplet, δ and α are assumed to be constant since the droplet is not a perfect prism or a cuboid, and W and H are the height and width of the microchannel, respectively. The value of the equivalent radius of the droplet was $(1.26 \times 10^2(\delta + \alpha))$ μm by using the above formula. Meanwhile, by using image processing, an image is displayed by using a microscope (Leica MZ16, Meyer Inc.) connected with a camera (WAT-221S, Watec Inc.); the droplet size was 1.23×10^2 μm. To explicitly calculate the droplet size by using two different calculation methods, i.e., image processing and microsensor, the calibration results are shown in **Fig. 16**. From this figure, it can be easily observed that the estimated sizes were nearly identical by using the two different calculation methods. Meanwhile, δ and α are estimated to be 0.9992 and 0.118, respectively, in Eq. (4). The droplet-size accuracy is given by radius $\pm 9.8\%$. The droplets could be detected, and the size could be calculated just by employing two pairs of electrodes in a simple way.

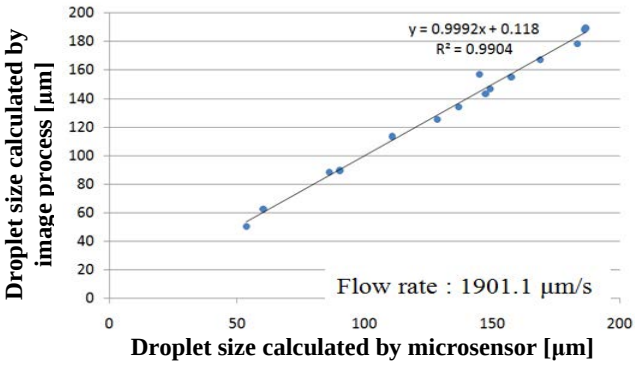

Fig. 16. Equivalent radius of droplet estimated by image processing and voltage signal calculation.

5. Conclusions

We have successfully produced size-controlled emulsion droplets on a chip by monitoring the frequency of MMT. A thin coplanar Au electrode was successfully fabricated on a substrate of the microchip to work as a capacitor, and this microsensor provided the droplet generation system with in-situ droplet detection. A change in capacitance was detected in real time, and we measured the microsensor output to estimate the droplet size. New driving signals can be manually set for MMT to achieve on-demand and size control of the droplet. On the basis of this principle, we will apply a real-time feedback controller to this system for demonstrating the stabilization of controlled droplet sizes. Through the expansion of closed-loop control with a microsensor, we can realize automatic generation of size-controlled droplets with a high accuracy.

Acknowledgements
This work is financially supported by JST-SENTAN.

References:

[1] C. Charcosset, I. Limayem, and H. Fessi, "The membrane emulsification process – a review," J. of Chemical Technology and Biotechnology, Vol.79, pp. 209-218, 2004.

[2] A. V. Korobko, W. Jesse, and J. R. C. Van der Maarel, "Encapsulation of DNA by Cationic Diblock Copolymer Vesicles," Vol.21, pp. 34-42, 2005.

[3] S. M. Moghimi, A. C. Hunter, and J. C. Murray, "Nanomedicine: current status and future prospects," The FASEB Journal, Vol.19, pp. 311-330, 2005.

[4] T. Kojima, Y. Takei, M. Ohtsuka, Y. Kawarasaki, T. Yamane, and H. Nakano, "PCR amplification from single DNA molecules on magnetic beads in emulsion: application for high-throughput screening of transcription factor targets," Nucleic Acids Research, Vol.33, Vol.17, e150, 2005.

[5] C-W. Lai, Y-H. Lin, and G-B. Lee, "A microfluidic chip for formation and collection of emulsion droplets utilizing active pneumatic micro-choppers and micro-switches," Biomedical Microdevices, Vol.10, pp. 749-756, 2008.

[6] R. Heusch and B. A. G. Leverkusen, "Ullmann's Encyclopedia of Industrial Chemistry," 2000.

[7] B. Zheng, J. D. Tice, and R. F. Ismagilov, "Formation of arrayed droplets by soft lithography and two-phase fluid flow, and application in protein crystallization," Adv. Mater., Vol.16, No.15, pp. 1365-1368, 2004.

[8] G. Yi, T. Thorsen, V. N. Manoharan, M. Hwang, S. Jeon, D. J. Pine, S. R. Quake, and S. Yang, "Generation of uniform colloidal assemblies in soft microfluidic devices," Adv. Mater., Vol.15, No.15, pp. 1300-1304, 2003.

[9] G. Yi, S. Jeon, T. Thorsen, V. N. Manoharan, S. R. Quake, D. J. Pine, and S. Yang, "Generation of uniform photonic balls by template-assisted colloidal crystallization," Synth. Met. 139, pp. 803-806, 2003.

[10] D. Dendukuri, K. Tsoi, T. A. Hatton, and P. S. Doyle, "Controlled synthesis of nonspherical microparticles using microfluidics," Langmuir, Vol.21, pp. 2113-2116, 2005.

[11] T. Nisisako, T. Torii, and T. Higuchi, "Novel microreactors for functional polymer beads," Chem. Eng. J., Vol.101, pp. 23-29, 2004.

[12] J. Lee and C. Kim, "Surface-tension-driven microactuation based on continuous electrowetting," J. Microelectromech. Syst., Vol.9, No.2, pp. 171-180, 2000.

[13] S.-K. Chae, C.-H. Lee, S. H. Lee, T.-.S Kim, and J. Y. Kang, "Oil droplet generation in PDMS microchannel using an amphiphilic continuous phase," Lab Chip, Vol.9, pp. 1957-1961, 2009.

[14] C.-H. Lee, S.-K. Hsiung, and G.-B. Lee, "An Active Flow Focusing Microfluidic Chip Utilizing Controllable Moving Walls for the Formation of Microdroplets in Liquid," Proc. of the 2nd IEEE Int. Conf. on Nano/Micro Engineering and Molecular systems, Bangkok, Thailand, pp. 167-171, 2007.

[15] T. Schneider, D. R. Burnham, J. VanOrden, and D. T. Chiu, "Systematic investigation of droplet generation at T-junctions," T. Schneider, D. R. Burnham, J. VanOrden and D. T. Chiu (Eds.), Lab Chip, Vol.11, pp. 2055-2059, 2011.

[16] S. Y. Park, T. H Wu, Y Chen, M. A. Teitell and P. Y Chiou, "High-speed droplet generation on demand driven by pulse laser-induced cavitation", Lab Chip, Vol.11, p. 1010-1012, 2011.

[17] M. Hagiwara, T. Kawahara, Y. Yamanishi, and F. Arai, "Driving Method of Microtool by Horizontally-arranged Permanent Magnets for Single Cell Manipulation," Applied Physics Letters, Vol.97, 013701, pp. 013701-1-013701-3, 2010.

[18] Y. Yamanishi, S. Sakuma, K. Onda, and F. Arai, "Powerful Actuation of Magnetized Microtools by Focused Magnetic Field for Particle Sorting in a Chip," Biomed Microdevices, Vol.12, pp. 745-752, 2010.

[19] D. R. Link, S. L. Anna, D. A. Weitz, and H. A. Stone, "Geometrically Meditated Breakup of Drops in Microfluidic Devices," Physical Review Letter, Vol.92, No.054503, 2004.

[20] J. Z. Chen, A. A. Darhuber, S. M. Troian, and S. Wagner, "Capacitive sensing of droplets for microfluidic devices based on thermocapillary actuation," Lab on a Chip. Jun; Vol.6, No.6, pp. 744-751, 2006.

Name:
Lin Feng

Affiliation:
Ph.D. Student, Department of Micro-Nano Systems Engineering, Nagoya University

Address:
Furo-cho, Nagoya 464-8603, Japan

Brief Biographical History:
2008 B.S. in School of Geophysics and Geoinformation Systems, China University of Geosciences, China
2011 M.S. degree in Department of Biorobotics, Tohoku University
2011- Ph.D. Student, Department of Micro-Nano Systems Engineering, Nagoya University

Main Works:
• M. Hagiwara, T. Kawahara, Y. Yamanishi, T. Masuda, L. Feng, and F. Arai, "On-Chip Magnetically Actuated Robot with Ultrasonic Vibration for Single Cell Manipulations," Lab on a Chip, Vol.11, Issue 12, pp. 2049-2054, 2011.
• Y. Yamanishi, L. Feng, and F. Arai, "On-demand Production of Emulsion Droplets Over a Wide Range of Sizes," Advanced Robotics, Vol.24, No.14, pp. 2005-2018, 2010.

Membership in Academic Societies:
• The Robotics Society of Japan (RSJ)
• The Japan Society of Mechanical Engineers (JSME)

Name:
Tomohiro Kawahara

Affiliation:
Assistant Professor, Department of Micro-Nano Systems Engineering, Nagoya University

Address:
Furo-cho, Nagoya 464-8603, Japan

Brief Biographical History:
2006 Dr. of Eng. from Hiroshima University
2006- Post Doctoral Researcher, Hiroshima University Hospital
2010- Assistant Professor, Tohoku University
2010- Assistant Professor, Nagoya University

Main Works:
• M. Hagiwara, T. Kawahara, Y. Yamanishi, and F. Arai, "Driving Method of Microtool by Horizontally-arranged Permanent Magnets for Single Cell Manipulation," Applied Physics Letters, Vol.97, 2010.
• T. Kawahara, Y. Miyata, K. Akayama, M. Okajima, and M. Kaneko, "Design of Noncontact Tumor Imager for Video-Assisted Thoracic Surgery," IEEE/ASME Trans. on Mechatronics, Vol.15, No.6, pp. 838-846, 2010.
• T. Kawahara, S. Tanaka, and M. Kaneko, "Non-Contact Stiffness Imager," The Int. J. of Robotics Research, Vol.25, No.5-6, pp. 537-549, 2006.

Membership in Academic Societies:
• The Robotics Society of Japan (RSJ)
• The Japan Society of Computer Aided Surgery (JSCAS)
• The Society of Instrument and Control Engineers (SICE)
• The Institute of Electrical and Electronics Engineers (IEEE) Robotics and Automation Society (RAS)
• The Japan Society of Mechanical Engineers (JSME)
• The Japan Society of Medical Electronics and Biological Engineering (JSMBE)

Name:
Yoko Yamanishi

Affiliation:
Associate Professor, Nagoya University, Department of Micro-Nano Systems Engineering, Department of Mechanical Science and Engineering, Nagoya University

Address:
Furo-cho, Nagoya 464-8603, Japan

Brief Biographical History:
2003 Ph.D. in Engineering, Imperial College London
2004- Lecturer, Shibaura Institute of Technology
2006- Post Doctoral Researcher, Tohoku University
2008- Assistant Professor, Tohoku University
2009- JST PRESTO Researcher
2011- Associate Professor, Nagoya University

Main Works:
• Y. Yamanishi, S. Sakuma, K. Onda, and F. Arai, "Powerful Actuation of Magnetized Microtools by Focused Magnetic Field for Particle Sorting in a Chip," Biomedical Microdevices, Vol.12, pp. 745-752, 2010.
• Y. Yamanishi, S. Sakuma, Y. Kihara, and F. Arai, "Fabrication and Application of 3D Magnetically Driven Microtools," J. of Microelectromechanical Systems, Vol.19, No.2, pp. 350-357, 2010.
• Y. Yamanishi, J. Teramoto, Y. Magariyama, A. Ishihama, T. Fukuda, and F. Arai, "On-chip Cell Immobilization and Monitoring System Using Thermosensitive Gel Controlled by Suspended Polymeric Microbridge," IEEE Trans. on NanoBioscience, Vol.8, No.4, pp. 312-317, 2009.

Membership in Academic Societies:
• The Japan Society of Mechanical Engineers (JSME)
• The Robotics Society of Japan (RSJ)
• IEEE Robotics and Automation Society (RAS)

Name:
Kazuhiro Kosuge

Affiliation:
Professor, Department of Bioengineering and Robotics, Tohoku University

Address:
6-6-01 Aza-aoba, Aramaki, Aoba-ku, Sendai 980-8579, Japan

Brief Biographical History:
1980- Research Staff, DENSO Corporation
1982- Research Associate, Tokyo Institute of Technology
1988 Doctor of Engineering, Tokyo Institute of Technology
1989- Visiting Research Scientist, Massachusetts Institute of Technology
1990- Associate Professor, Nagoya University.
1995- Professor, Tohoku University

Main Works:
• M. Shimizu, H. Kakuya, W.-K. Yoon, K. Kitagaki, and K. Kosuge, "Analytical Inverse Kinematic Computation for 7-DOF Redundant Manipulators With Joint Limits and Its Application to Redundancy Resolution," IEEE Trans. on Robotics, Vol.24, No.5, pp.1131-1142, 2008.
• K. Kosuge, T. Takeda, and Y. Hirata, "A Robot Waltzing with a Human Partner – Dance Partner Robot – [Trends and Controversies: Dnacing Robots]," IEEE Intelligent Systems, Vol.23, No.2, 2008.

Membership in Academic Societies:
• IEEE Robotics and Automation Society (RAS)
• The Robotics Society of Japan (RSJ)
• Japan Society of Mechanical Engineers (JSME)
• Society of Instrument and Control Engineers (SICE)
• Institute of Systems, Control and Information Engineers (ISCIE)
• Institute of Electrical Engineers of Japan (IEEJ)

Name:
Masaya Hagiwara

Affiliation:
Ph.D. Student, Department of Micro-Nano Systems Engineering, Nagoya University

Address:
Furo-cho, Nagoya, Aichi 464-8603, Japan

Brief Biographical History:
2005 M.S. degree in Department of Mechanical Engineering, University of Kentucky, U.S.A.
2005- Production Engineer, Toyota Motor Corporation
2009- Ph.D. Student, Department of Bioengineering and Robotics, Tohoku University
2010- Ph.D. student, Department of Mechanical Science & Engineering, Nagoya University
2011- Research Fellow (DC2) at Japanese Society for the Promotion of Science

Main Works:
• M. Hagiwara, T. Kawahara, Y. Yamanishi, T. Masuda, L. Feng, and F. Arai, "On-Chip Magnetically Actuated Robot with Ultrasonic Vibration for Single Cell Manipulations," Lab on a Chip, Vol.11, Issue 12, pp. 2049-2054, 2011.
• M. Hagiwara, T. Kawahara, Y. Yamanishi, and F. Arai, "Driving Method of Microtool by Horizontally-arranged Permanent Magnets for Single Cell Manipulation," Applied Physics Letters, Vol.97, 2010.

Membership in Academic Societies:
• The Japan Society of Mechanical Engineers (JSME)
• The Robotics Society of Japan (RSJ)
• IEEE Robotics and Automation Society (RAS)

Name:
Fumihito Arai

Affiliation:
Professor, Department of Micro-Nano Systems Engineering, Nagoya University

Address:
Furo-cho, Nagoya 464-8603, Japan

Brief Biographical History:
1989- Research Associate, Nagoya University
1993 Dr. of Engineering from Nagoya University
1994- Assistant Professor, Nagoya University
1998- Associate Professor, Nagoya University
2005- Professor, Tohoku University
2010- Professor, Nagoya University

Main Works:
• F. Arai, C. Ng, H. Maruyama, A. Ichikawa, H. El-Shimy, and T. Fukuda, "On Chip Single-Cell Separation and Immobilization Using Optical Tweezers and Thermo Sensitive Hydrogel," Lab on a chip, Vol.5, No.12, pp.1399-1403, 2005.
• T. Fukuda, F. Arai, and L. Dong, "Assembly of Nanodevices with Carbon Nanotubes through Nanorobotic Manipulations," Proc. of the IEEE, Vol.91, No.11, pp. 1803-1818, 2003.

Membership in Academic Societies:
• The Japan Society of Mechanical Engineers (JSME)
• The Robotics Society of Japan (RSJ)
• IEEE Robotics and Automation Society (RAS)